MDPI

Article

Fan Fault Diagnosis Using Acoustic Emission and Deep Learning Methods

Giuseppe Ciaburro [1,*], Sankar Padmanabhan [2], Yassine Maleh [3] and Virginia Puyana-Romero [4,5]

1 Department of Architecture and Industrial Design, Università degli Studi della Campania Luigi Vanvitelli, 81031 Aversa, Italy
2 Department of Electronics and Communication Engineering, Hindustan Institute of Technology and Science, Chennai 603103, TN, India
3 Ecole Nationale des Sciences Appliquée (ENSA) Khouribga, Sultan Moulay Slimane University, Beni Mellal 25000, Morocco
4 Department of Sound and Acoustic Engineering, Universidad de Las Américas, Quito EC170125, Ecuador
5 Laboratory of Phonetics and Acoustics, Institute of Applied Linguistics, Universidad de Cádiz, 11002 Cádiz, Spain
* Correspondence: giuseppe.ciaburro@unicampania.it

Abstract: The modern conception of industrial production recognizes the increasingly crucial role of maintenance. Currently, maintenance is thought of as a service that aims to maintain the efficiency of equipment and systems while also taking quality, energy efficiency, and safety requirements into consideration. In this study, a new methodology for automating the fan maintenance procedures was developed. An approach based on the recording of the acoustic emission and the failure diagnosis using deep learning was evaluated for the detection of dust deposits on the blades of an axial fan. Two operating conditions have been foreseen: No-Fault, and Fault. In the No-Fault condition, the fan blades are perfectly clean while in the Fault condition, deposits of material have been artificially created. Utilizing a pre-trained network (SqueezeNet) built on the ImageNet dataset, the acquired data were used to build an algorithm based on convolutional neural networks (CNN). The transfer learning applied to the images of the spectrograms extracted from the recordings of the acoustic emission of the fan, in the two operating conditions, returned excellent results (accuracy = 0.95), confirming the excellent performance of the methodology.

Keywords: deep learning; transfer learning; acoustics emission; fault diagnosis

1. Introduction

Today, indoor air quality is a topic that is being given massive attention. The concentration and definition of the primary pollutants found in the built environment are directly related to the main issues with Indoor Air Quality (IAQ) [1]. Energy conservation has forced greater insulation of buildings resulting in lower ventilation rates, and the use of new materials and equipment: solutions that increase concentrations of pollutants [2]. The quality of air in the built environments has been steadily declining over the previous few decades. Various scientific research has shown that there are contaminants in the air in homes at low concentrations that are difficult to quantify and can have health impacts [3–5]. Environmental discomfort is decreased, and health risks result from indoor pollution. Chemical (organic and inorganic substances), physical (ionizing and non-ionizing radiation), and biological contaminants can all be included in this category (microorganisms, molds, mites). Exposure to indoor pollution predominates in comparison to exposure to outdoor pollution since a substantial portion of the population spends their time in enclosed environments [6].

A growing body of research has shown that indoor pollution increases the chance of developing respiratory disease, most likely due to airway inflammation caused by oxidative

stress processes [7]. In addition, the main trigger of sensitization and aggravation in asthma patients are indoor allergens [8]. Currently, the problem has assumed greater relevance due to the current COVID-19 pandemic which has highlighted the problems of spreading the disease [9–11]. The ways in which biological agents can spread in a confined environment are essentially the following: direct, indirect, and airborne transmission [12,13]. In airborne transmission, there is a dissemination of the biological agent, in the form of small particles large enough to be inhaled, which maintains its infective capacity over time and space. Microorganisms can be carried great distances by air currents and be inhaled by the host. Building Related Illness (BRI) is a symptomatology that comprises infectious diseases (caused by bacteria, fungi, and viruses) as well as allergy diseases (allergic alveolitis, asthma, and legionella), all of which are brought on by the cumulative long-term effects of toxic substances [14,15]. Sick Building Syndrome (SBS) is a symptomatology that has been statistically proven to affect groups of people who operate primarily in buildings with air conditioning systems. SBS symptoms include respiratory, ocular, cutaneous, neuropsychiatric, and unpleasant odor manifestations [16,17].

One of the most important sources of indoor pollution is from air conditioning systems [18]. They act as incubators for germs and receptacles for colonies of molds, yeasts and bacteria, whose spores cause many allergies and bronchopneumonia. This phenomenon also generates microbial spread within the confined environment, that is, a rapid and endemic increase in contagions among users of the same building, air-conditioned in all its parts by the same system [19]. The spread of biological agents is due to the need for these systems to move previously conditioned air, which results in their transmission by air [20]. An essential element in the movement of air flows is the fan [21]. In addition to imposing the movement of the air, the fan can itself act as a source of diffusion of the biological agent [22]. This is because material deposits on the blades of the fan over time, which becomes an ideal place for the proliferation of infectious agents. In order to prevent these agents from being airborne to the occupants of the confined space over time, appropriate maintenance interventions must be planned to ensure that equipment is cleaned and sanitized [23].

The concept of maintenance expresses the need to preserve and maintain equipment in a fully efficient state. Put in this way, maintenance activity seems to be limited to the simple corrective action that must be performed in case of failure [24]. In such a case, the necessary maintenance action is aimed at repairing the entity and restoring the initial operating conditions in the shortest possible time. Alternatively, and often to prevent corrective maintenance activities, other maintenance modes can then be adopted that seek to avoid the occurrence of the failure by predicting and correcting it before it occurs. However, this type of maintenance, unlike corrective maintenance, is not so intuitive; rather, before it can be implemented it requires a careful study of the type and cause of the failure to which the equipment is subjected [25]. In the present case, we are interested in preventing the deposition of material on the surface of the fan blades, which, as mentioned above, becomes a place for the proliferation of pathogens. In this sense, it is necessary to identify a methodology that can uniquely identify this condition.

In an air handling system, it is the fan that emits the most noise [26]. The problem can be exacerbated by the superimposition of secondary noise generated by the system itself, such as the forced passage of air through ducts, vents, and grilles [27]. Fan noise has a mechanical origin and an aerodynamic origin [28]. Mechanical noise is caused by the structural radiation of the motor block, and other related parts, resulting from the stress of fluctuating forces related to both the rotating parts and the turbulence of the airflow [29]. Aerodynamic noise is determined by the periodic impulses that each impeller blade imparts to the nearby air and by the contributions originated by vortices in the turbulent wake of the blades [30]. The deposition of material on the blade surface results in a substantial change in its aerodynamics, which alters its acoustic emission. However, this does not result in a change that can be evaluated by common sound analysis techniques.

Recently, techniques based on machine learning have been widely used in the scientific community for fault identification [31–34]: The objective is to be able to gather as much information as possible on the condition of machinery in the real time, often using sensors, and to correlate it with the rate of component deterioration or system performance. Algorithms based on Machine Learning automatically extract knowledge from data thanks to the data inputs received, without the need for specific commands from the developer [35–38]. As is typical of artificial intelligence, in these models the computer can decide for itself which patterns to follow to produce the intended outcome. The system gets a collection of data required for training, calculating the relationships between the input data and the output data, in the learning process that distinguishes various algorithms. These connections represent the model's parameters that the system has estimated [39–43]. Xu et al. [44] used an algorithm based on extreme machine learning for fan failure diagnosis. To simulate the failure, they drilled holes in the blade of an axial fan, thus resulting in rotor imbalance. The impeller vibration signals were collected and sent to the classifier to identify the rotor misalignment error. Huang et al. [45] have exploited four different algorithms based on Machine Learning to diagnose fan failures of an axial fan. ANN, SVM, KNN, and RFE were used returning different results, from their comparison the ANN-based classifier returned the best performance in recognizing failures of the artificially created fan blades. Four different types of fan failures were artificially induced: a hole in the blade, a break in the blade, a vertical and horizontal crack. Zhang et al. [46] exploited both acoustic and vibrational emission signals to train a one-dimensional convolutional neural network to identify damage to a centrifugal fan blade. The multi-source signals were first fused through a weighted methodology with adaptive data synchronization. CNN then extracts the characteristic from the signals and uses them for damage recognition. Xie et al. [47] used the vibration signals of four centrifugal fan blade failure states. For the feature extraction the authors adopted the refined generalized multiscale entropy. The features were then used as input for a Support Vector Machine obtaining good results in fault classification.

A defect in a fan blade causes an imbalance that affects the rotation around its axis. Choudhary et al. [48] used infrared thermography coupled with ML-based algorithms to identify bearing failures in induction motors. The infrared thermal image of the bearings in use was subjected to the two-dimensional discrete wavelet transform by the authors. Prior to the implementation of various classifiers based on the complex decision tree, linear discriminant analysis, and support vector machine for fault identification, principal component analysis allowed for the reduction of the dimensionality of the extracted data. Hsu et al. [49] have developed an automatic system for detecting wind turbine failures based on the data collected by the sensors for monitoring the rotation speed, temperature, and voltage at the nacelle. The system also provides tools for predicting plant maintenance needs. Rauber et al. [50] implemented an experimental methodology to evaluate failures from vibration signals based on ML. The authors used one-dimensional convolutional neural networks, support vector machines, nearest neighbor K classifier, random forests, and Case West-ern Reserve University survey data [51] to diagnose satellite faults using ML. Remote control of the satellites takes place based on telemetry data collected in real time, resulting in a quantity of data (Big Data) that is difficult to monitor, at least for the human eye. However, these data represent a significant source of information that can be extracted with the use of ML. Using the telemetry parameters of the Egyptsat-1 satellite, which was launched in April 2007 and unplugged because of a defect in 2010, the authors were able to identify the satellite's flaws.

In this work, a methodology for the detection of dust deposits on the blades of an axial fan was implemented through acoustic emission acquisition and fault identification based on Deep Learning. First, the data relating to the different operating conditions were collected. Two operating conditions have been identified: No-Fault, Fault. In the No-Fault condition, the fan blades are perfectly clean and there are no accumulations of material on the surface. In the Fault condition, on the other hand, deposits of material have been artificially created on the fan blades to simulate those normally found in the normal

operation of the equipment. Through a dichotomous categorization, the measurements of the fan's acoustic emission in the various operating circumstances have been appropriately classified (No-Fault, Fault). The gathered information was utilized to train a convolutional neural network (CNN) algorithm for the automatic recognition of the fan's operating characteristics. The paper is set up like follows: The properties of the fan and the process used to collect data are both covered in detail in Section 2. In addition, the approaches for feature extraction and algorithm training based on deep learning are discussed. The outcomes of using this methodology are shown in Section 3, along with a summary of its advantages and a list of its drawbacks. Section 4 concludes by summarizing the findings of this investigation.

2. Materials and Methods

In this study, a procedure for the automatic identification of the operating conditions of a fan was developed. As a result, the system signals the state of the material deposited on the fan blades in order to schedule adequate maintenance (Figure 1).
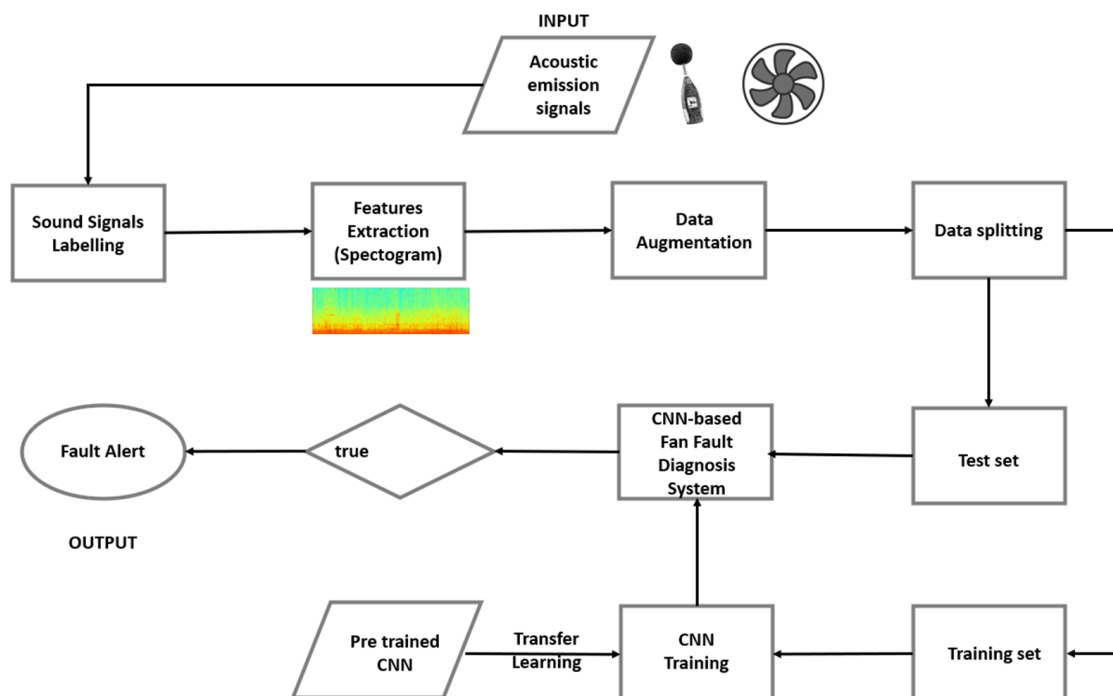

Figure 1. Flow chart of the automated system for fan fault diagnosis.

The procedure described in Figure 1 can signal in advance the need for maintenance intervention to remove the dust deposits on the fan blades. In this way we intervene only when necessary, avoiding interrupting production if not requested.

2.1. Introduction to Fan Systems

A fan is a rotating machine that employs mechanical energy to maintain an uninterrupted flow of air at a fixed pressure without changing its density using one or more blades. Therefore, the primary function of a fan is to circulate a specific volume of air at a pressure high enough to overcome the resistance of the system it is attached to. Different types and sizes of fans can be employed for a particular flow and pressure demand.

The selection of the most appropriate fan for each case must therefore be carried out considering factors such as the space occupied, the type of motor with which to power it, the noise level, the mechanical and aerodynamic efficiency, the mechanical resistance and, finally, the cost [52].

Fans are classified into two main types, depending on their construction design: centrifugal and axial fans. In the axial fans (Figure 2) the air flow passes through the fan blades essentially in a direction parallel to the rotation axis of the impeller, keeping the average flow direction unchanged, despite the onset of whirling phenomena due to the rotation of the blades. The major component of the force applied by the blades is in the axial direction from the inlet to the outlet, which causes an increase in pressure. The main characteristics of an axial fan strongly depend on the number of blades and on the angle of these with respect to the flow. These fans are more suitable for situations with a high ratio between flow and pressure.
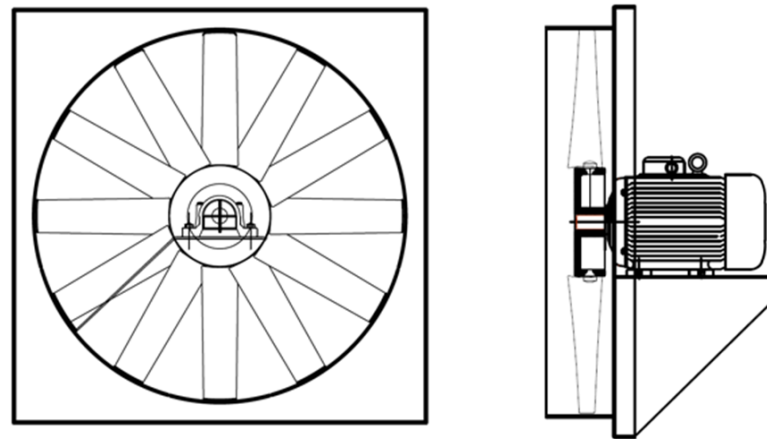
Figure 2. Axial fan scheme (front and side view).

Axial fans tend to rotate with a higher speed at the tip of the blades than their centrifugal counterpart for the same performance, tending to be noisier. They are also more affected by blade stall phenomena. In contrast, they may be joined in series or parallel configurations of many fans, are more compact than centrifugal fans, and readily change the direction of flow by simply changing the direction of spin. They are also more suitable for handling large flow rates. Centrifugal fans, on the other hand, have greater performance for high operating pressures. In this work, an axial fan was studied, a very common type in the ventilation of confined spaces.

2.2. The Noise Made by a Fan

The noise produced by the fans can essentially be divided into two main contributions: mechanical and aerodynamic. Mechanical noise is produced by the structural radiation of the engine block, and of other connected parts, resulting from the solicitation of fluctuating forces linked both to the rotating parts and to the turbulence of the air flow [26]. The acoustic emission due to mechanical noise can be attenuated by using joints and anti-vibration supports and by adding foundation weights to reduce the vibrations of the structure. Aerodynamic noise is due to the periodic impulses that each blade conveys to the air and by contributions due to vortices in the turbulent wake of the air flow near the blades. The first contribution is produced by the rotation of the blades that make up the fan and is the result of the pressure fluctuations caused by the periodic variations of the forces in the fluid. This type of noise is caused by the thrust and drag forces present on the blades moving in the air, by the impulsive interaction of the blades with the incoming flow that is not perfectly straight, and by the interaction with any nearby obstacles [27]. Given the regularity of the passage of the blades near the obstacles, the noise emitted is a tonal noise, with a single frequency (Blade Passing Frequency—*BPF*) described by Equation (1).

$$BPF = z \times n,\qquad(1)$$

In the Equation (1) the terms have the following meaning:

- z = number of blades
- n = rotation frequency of the fan shaft.

The contribution to aerodynamic noise due to vortices is caused by a series of random forces caused by non-stationary fluid fields, by turbulence and by its interaction with rigid structures encountered by the flow. These forces may be due to the widening and narrowing of the passages where the fluid flows, asymmetries of the system, the impact of the flow on obstacles such as blades, and the respective formation of vortices. This type of noise is caused by the fluctuation of fluid forces in the time and frequency domains, and depends mainly on the flow velocity, the fan design, and the size and roughness of the sections [28].

Aerodynamic noise has the greatest influence on total noise. In very large machines, however, mechanical noise becomes more significant. The main mechanisms of aerodynamic noise generation can be summarized as follows:

- Vortex shedding noise: due to the diffusion of vortices, a solid's time-varying circulation creates a fluctuating force that is transferred to the fluid and propagates as sound;
- Interaction between turbulence and the solid structure: the presence of vortices in contact with a solid body induces oscillating forces acting on the surface of the same, due to the time-varying nature of the vortices. These are transferred to the fluid and propagated in the form of pressure waves and therefore noise;
- Trailing edge noise: it results from the interaction between the boundary layer instabilities and the blade edges, which is typical of rotating devices.

It follows that the shape of the blades in a fan significantly influences the acoustic emissions and characterizes its noise. The deposit of material on the blades of a fan, effectively changing its shape, therefore determines a variation of its acoustic emission. The purpose of this work is to acoustically characterize this operating condition of the fan to be able to identify it automatically.

2.3. Maintenance of a Fan

The fan blades act as attractors of dust and more generally of all the substances with which they come into contact. As they move, the blades are charged with static electricity due to the friction created by the cutting of the air. In this way, the dust particles present in the environment accumulate on the surfaces of the blades. The location of the fan determines the amount of dust that can settle on the fan blades. The deposit is greatest at the leading edges of the fan blade, as this is where static electricity generation is greatest. These accumulated dust particles attract even more dust particles as they remain there over time, this therefore increases the time the dust stays on the fan blades [53].

The blades of a fan not only accumulate dust but can later also spread it. Dusty and dirty fans can expel dust and biological agents in general into the air. Regular cleaning of the fan not only ensures dust-free blades, but also keeps the equipment in good working order. An excessive accumulation of dust can in fact affect the performance and efficiency of the fan. Particles of dust can in fact penetrate the mechanism of the fan motor and damage it: Improperly functioning fans can consume more energy and reduce the flow of treated air, furthermore the continuous interruption of the fan mechanisms could lead to the final break [54].

For proper operation of the device, it is therefore necessary to remove the deposit of material on the blades of a fan. Periodic cleaning of the impeller avoids vibrations caused by any deposits of dust accumulated during fan operation. If the fan is intended for the treatment of even slightly dusty fluids, containing abrasive powders, it is necessary to periodically inspect the state of cleanliness and/or wear of the impeller. This operation can be carried out, after a prior visual inspection which reveals the need, with a thorough cleaning carried out with suitable detergents. Or it can be programmed through the adoption of a maintenance plan which carries out the interventions to remove the deposits, at a time interval calculated based on the technical information available on the accumulation

capacity of the material on the blades. However, problems arise when such information is not available, or when the characteristics of the fluid to be treated are not constant over time [55]. Furthermore, cleaning the blades is not always an easy operation. Think of the case in which the fan is not immediately visible in the system, and in the case in which to access it is necessary to provide for the temporary shutdown of the system and the disassembly of its components: In these cases, not even a visual inspection is guaranteed. In these cases, it is necessary to develop an automated procedure which makes it possible to identify the state of cleanliness and/or wear of the impeller.

2.4. Measurements of the Acoustic Emission of the Fan Blades

Dust deposits on the fan blades determine a variation in the aerodynamic profile with consequent modification of the noise produced. In this work, measurements of the acoustic emission of a three-blade axial fan have been carried out, to identify the different operating conditions.

Two operating conditions have been made:

- No-Fault: the fan blades have been perfectly cleaned and no accumulations of material have been foreseen on the surface;
- Fault: deposits of material have been artificially made on the fan blades to simulate those that normally occur in the normal operation of the equipment.

Acoustic tests were made in an anechoic chamber (4.40 m 4.40 m 4.50 m) for each of the two designs, with fiber-glass absorbing wedges and a cutoff frequency of 100 Hz: Consequently, there is a large reduction in the signals' reflection off of the walls (Figure 3). This method of measurement has no issues in the case of rotating blades because it does not necessitate physical contact between the sensor and the moving object, as is necessary for the detection of vibrations. The fan was positioned in the center of the anechoic chamber to produce a fixed source-receiver system, eliminate positioning error, and achieve good signal capture in order to simulate the operational conditions.

Figure 3. Set up of measurements in an anechoic chamber. The decision to place the sound level meter behind the fan was made to avoid the influence of the air flow on the measurement.

The Class 1 integrated sound level meter model 01 dB Black Solo that complies with UNI EN ISO 3745:2012 was used to conduct the acoustic measurements [56]. The sound

level meter was placed on a tripod at the same height as the fan in three positions with a radius of 1.2 m, the fan in the middle, and the positions set at staggered angles of 90 degrees to accurately characterize the acoustic emission of the fan (Figure 2). The data collected was used to train an algorithm based on CNNs for the automatic identification of the fan operating conditions.

2.5. Feature Extraction

To extract the features that could be used to determine the damage, the recorded audio signals were analyzed. This is an essential phase for the identification of damages; in fact, the extracted descriptors will be exploited as input both in the training phase of the classifier and in the subsequent testing phase [57]. We have already highlighted that the discrimination between state of health and state of damage in a fan is a complex task that cannot be treated simply with the identification of sound triggers that can identify the two operating conditions. An analysis in the time domain would prove inadequate to discriminate between the two states of the fan. To assess the energy levels in the various frequencies, we must consequently move our study into the frequency domain. To accomplish this, we can use the Fourier operator, which allows us to move from the time domain to the frequency domain by projecting the signal measured over time on an orthonormal basis of complex expressions [58]. In order to accurately complete the transition from the time domain to the frequency domain, the discrete Fourier transform (DFT) takes into account a sample of the signal over time located in a time window, we can calculate the complex component in the frequency domain with the Equation (2):

$$x_k = \frac{1}{N} \sum_{n=0}^{N-1} x_n e^{2nk\frac{n}{N}} \tag{2}$$

Here,

- x_n nth sample of the signal
- N is the number of samples contained in the window
- k is the index of discrete frequencies.

The consequence of the DFT is a vector of complex numbers. The DFT assumes that the signal is stationary, but most of the signals change continuously, the audio signal is split into parts with a particular amount of overlap to get around this restriction, each of which is multiplied with the Hanning window such as to attenuate the beginning and end of segment. In this way, a the Short-Time Fourier Transform (STFT) is obtained which consists in dividing the signal into partially overlapping segments through a windowing operation and calculating the DFT of each segment. The STFT can be represented as a matrix of coefficients by arranging the DFT coefficients of each segment in different columns of a matrix, where the column index denotes time, and the row index denotes the frequency of the corresponding coefficient. The resulting matrix, known as a spectrogram, can be viewed as an image and displays the evolution of the signal in the time-frequency domain by computing the modulus of each coefficient. The spectrogram resulting from the STFT is also called linear spectrum because the amplitude varies linearly with frequency [59].

2.6. Fan Fault Diagnosis Based on CNN Model

A frequency domain study is necessary because ambient noise exhibits a wide variety of frequencies at various levels. The results of the frequency analysis are the energy levels in the various frequency bands, or the so-called signal spectrum, which is a Cartesian diagram of the sound's frequencies in relation to its energy content [60]. The signals detected by the operation of the fan in the anechoic chamber were previously treated for the extraction of the characteristics. The choice fell on the spectrogram which relates three essential variables in the representation of a sound: frequency, time, and intensity of the signal. To show these three variables in a two-dimensional diagram, a color map is used: Time is measured by the abscissa, frequency by the ordinate, and sound intensity by colors [61]. Dark colors on the color map denote low sound intensity, while light colors denote high sound intensity [61].

Dark colors on the color map denote low sound intensity, while light colors denote high sound intensity. To define the acoustic emission of the fan and find specific trends capable of differentiating between the two activities, it is important to employ the spectrogram to emphasize the instances of time in which frequency fluctuations occur.

A classifier based on CNNs was fed with the retrieved features (spectrogram of the two operating conditions) as input: due to their ability to recognize adjacency patterns through adaptive learning that progresses from the bottom level to the top level, CNNs have proven successful at characterizing data with a grid topology. They are highly helpful for object recognition in computer vision thanks to their characteristics [62]. The CNNs operate on raster images characterized by two-dimensional arrays in which each pixel assumes values in the range of 0 to 255: the adjacent pixels are interlaced with each other in defining a pattern that the CNNs associate with the weights of the network.

Technology name contains the essential feature of this type of Artificial Neural Network (ANN), the convolution operation, that is, the dot product between two matrices, a weight grid structure, and discover a comparable structure in the input [63]. Two-dimensional CNNs are therefore multilayer ANNs with at least one convolutional layer, to which an image is presented as input. RGB (RED, GREEN, BLUE) images are composed of a number of matrices that track the intensity of the basic colors in correspondence with each pixel. In this way, the traditional dimensions of an image (height and width) are now combined with a third: depth. The input layer will have these three dimensions and following layers with a multidimensional structure will be consistent with the independent features important for classification.

A CNN is a tightly connected ANN with convolution operation performed in the first layer: It works with grid structures with spatial relationships between cells, which identify small local regions passed from one layer to another. The results of the convolution operations carried out by the first layers define information matrices called activation, or characteristics map while the network's trainable parameters are tensors referred to as kernels.

The architecture of a CNN includes a sequence of the ensuing layers (Figure 4):

- Convolutional layer;
- Activation layer;
- Pooling layer;
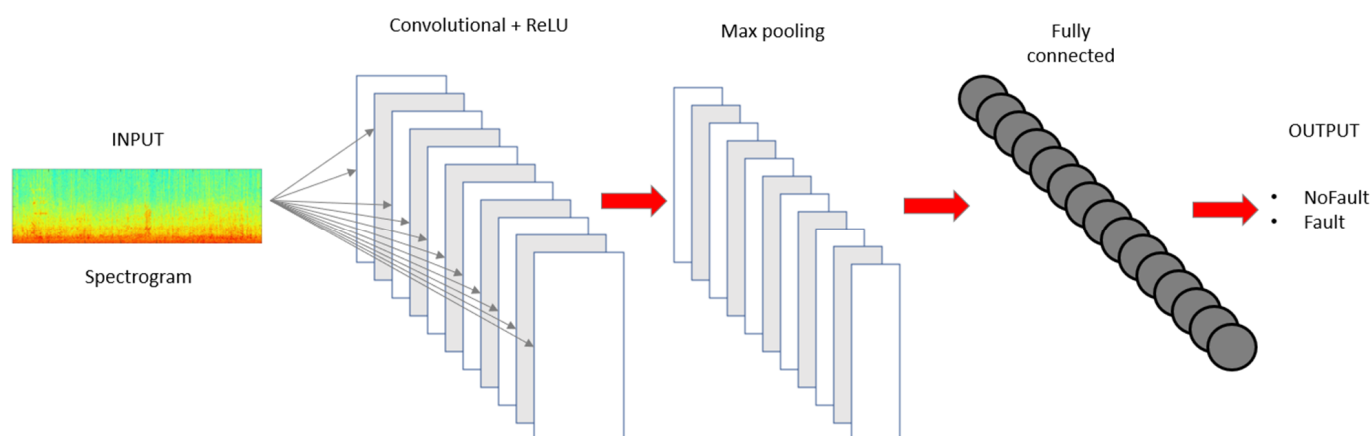- Densely connected layer.

Figure 4. CNN architecture for classification.

The convolution layer places a filter (kernel) in critical areas of the image and returns the scalar product of the kernel and the input matrix, or the "receptive field," which is a portion of the image that has the same proportions as the kernel [64]. The filter is moved by an amount equal to the stride until it hits the edge, at which point it convolves the entire image. Another matrix, known as a feature map, is created at the conclusion of the

scan and it focuses on a specific aspect of the image. Therefore, multiple filters are used simultaneously to perform the recognition, this will result in an output tensor whose depth equals the quantity of filters utilized. The activation operation that is nonlinear must be provided right after the convolution process. Each convolutional layer's activation function processes a layer of identical size with values constrained by thresholds [65].

The pooling level's objective is to resize the feature maps while maintaining the important properties. A filter of size 2 2 is typically employed in max pooling, and it moves on the feature map with steps that are the same size. The receptive fields are located by the pooling filter, which also determines the maximum value for each.

Finally, fully connected layers are subsequently added, which do the classification and produce the CNN output. The matrix that was altered by the levels before is fed into this layer of levels, which creates a vector of dimension N that equals the number of classes that need to be predicted.

2.7. Data Augmentation

Convolutional networks need many input data during training to give greater accuracy: Few images cause a more frequent analysis of the same during training, causing what is known as overfitting. Indicatively, a convolutional network begins to have an acceptable accuracy starting from a thousand images used for training. In cases where the acquisition of a large training dataset is complicated, there are techniques that allow to extract variations through artificial transformations of the images [66]. To enhance the quantity of training instances available we can apply the following transformations:

- Flipping;
- Cropping;
- Rotation;
- Translation;
- Distortion;
- Brightness change;
- Contrast adjustment.

These transformations must be chosen according to the images they must transform, this because the transformation must add information and must not introduce distortions [67]. For example, it is evident that the crop in our case is to be excluded as it would have stolen useful information, eliminating part of the spectrogram which instead represents the source of the features [68]. The general rule to consider is to maximize the variation of object transformations within each class and minimize the variation of transformations between different classes. The use of Data Augmentation causes slower model training convergence, which is irrelevant in the face of greater accuracy in testing [69].

2.8. Transfer Learning

A network initialized starting from random values requires some training time: The underlying principle of Transfer Learning is to reduce training times by exploiting networks that have already been trained for the recognition of objects with generic features [70]. The term Transfer Learning (TR) precisely means the possibility of adapting and transferring weights, to be able to use knowledge again to pursue many different objectives. Nearly all layers of the neural network are trained on a very large, generic dataset initially, allowing for the acquisition of global conceptions; thereafter, the specific dataset is utilized to train the remaining layers, and whether to propagate the errors through fine tuning is decided [71].

If on the one hand it is possible to reuse the knowledge of a neural network, it is still necessary to understand its specificity, above all in the case in which the final problem is not very similar to the starting one. The initial levels of a CNN deal with recognizing very generic features while those resulting from the final levels are more specialized and related to the dataset [72]. Furthermore, under some conditions, the transfer of weights can lead to a great improvement in the ability to generalize, increasing the overall accuracy of the CNN.

Pre-trained models are available from which specialized training can be continued. For small datasets it is advisable to allow modification of the final fully linked layers' properties, while for bigger datasets it is acceptable to modify the weights of the highest-level convolutional layers. The basic layers of the mesh usually extract features common to all objects, such as edges [73].

3. Results and Discussion

3.1. Characterization of the Acoustic Emission of the Fan

Beginning with an anechoic chamber (4.40 m 4.40 m 4.50 m), coated in absorbent glass fiber wedges, measurements of the fan's acoustic emission were made. The structure of the chamber's walls makes it feasible to minimize the reflection of signals on the walls: The chamber's cutoff frequency is 100 Hz.

The sound level meter was set up on a tripod at the same height as the fan and put on a pedestal in the middle of the room. The measurements were performed at three positions on a semicircle with a radius of 1.2 m, staggered at 90-degree angles, with the fan placed in its center [56]. There were three measurement sessions that were related to the three fan operating circumstances that corresponded to the three different fan speeds.

The diagram in Figure 5 shows that the acoustic emission levels measured in the lateral microphone positions are comparable to each other, while the measurements carried out in the microphone position at 270° show higher emission levels: As a result, this role is better suited to spotting any operational irregularities. The sound pressure levels (dB Lin) for the three fan speeds recorded at the three microphone sites are displayed in Table 1.
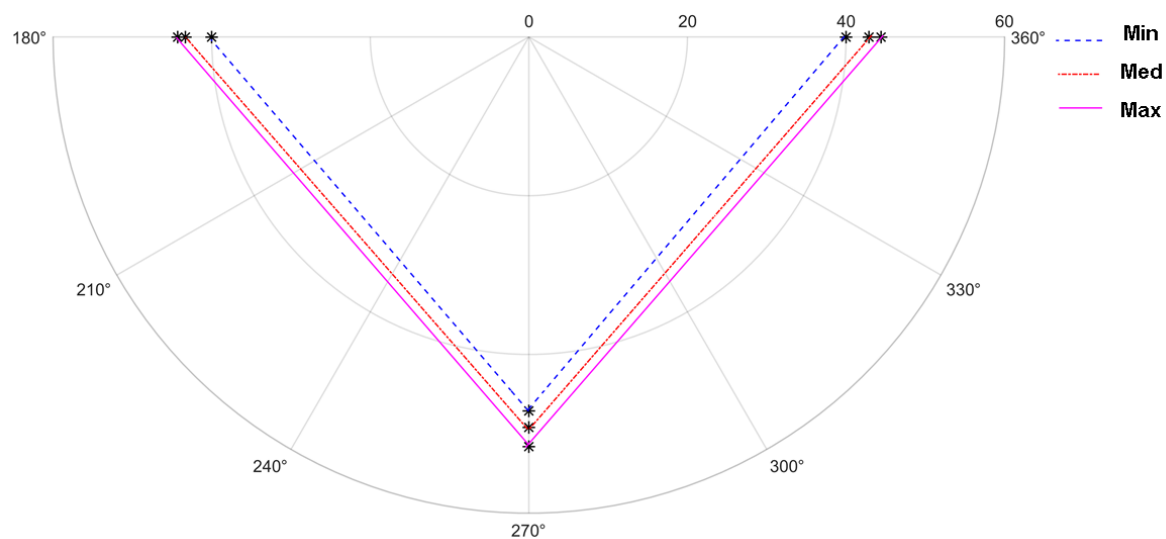

Figure 5. Sound pressure level (dB Lin) measured in the three microphone positions (180°, 270°, 360°) for the three operating conditions. The fan is positioned at the center with the airflow in the opposite direction to the microphone position 270°. The * represents the value of SPL at different microphone positions for the three operating conditions.

Table 1. Sound pressure level (dB Lin) measured.

Microphone Position	Min. Velox	Med. Velox	Max. Velox
180°	40.0	42.9	44.4
270°	47.1	49.2	51.6
360°	40.0	43.3	44.3

To describe how the fan functions, one must first step inside the frequency domain through a spectral analysis of the acoustic emission levels. Figure 6 shows the 1/3-octave

average spectral levels in the range of 20 Hz and 16 kHz for the three fan speeds and three measurement positions.
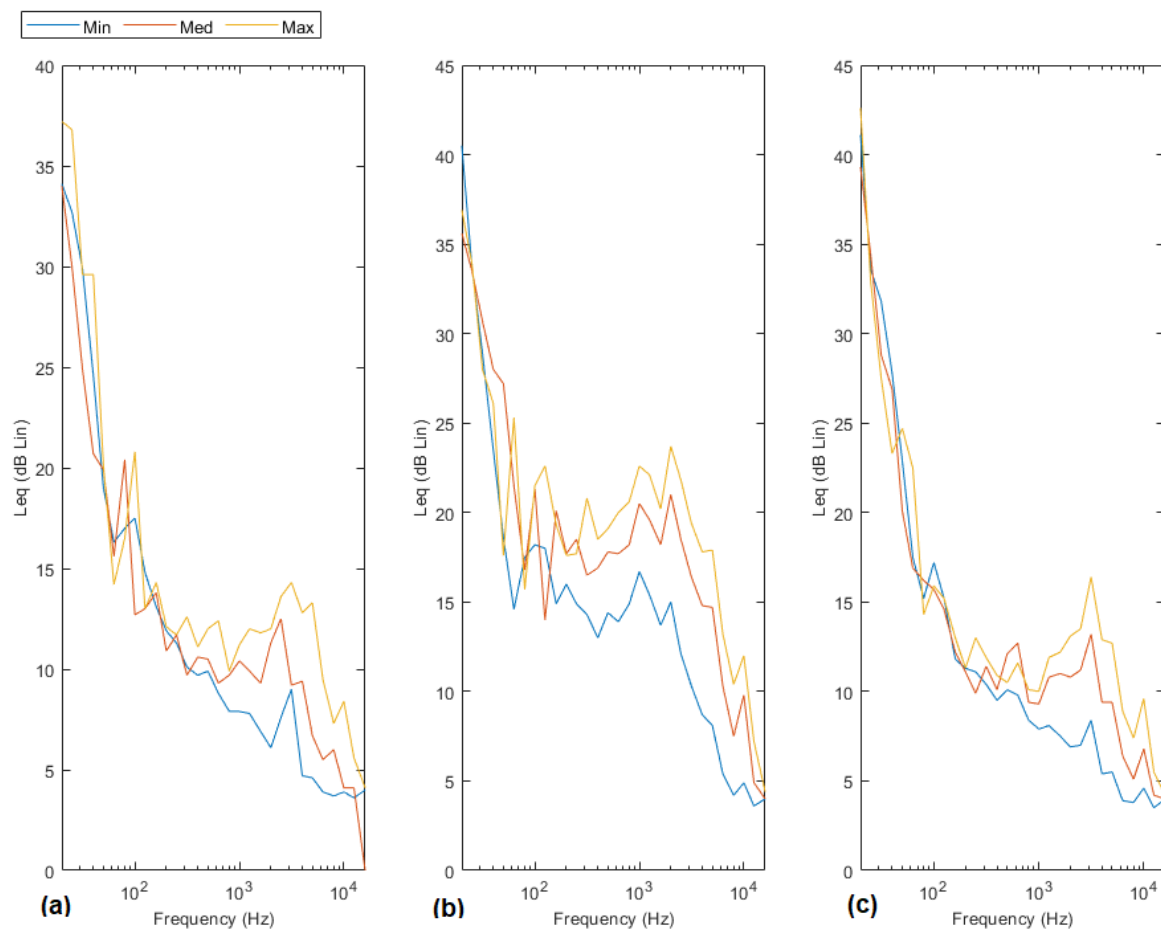

Figure 6. Spectral levels in a range spanning a third of an octave, 20 Hz to 16 kHz, for the three operating scenarios used in the measurement session at the three microphone placements (dB Lin). ((**a**): 180°, (**b**): 270°, (**c**): 360°).

Figure 6 shows that the energy content emitted at low frequencies characterizes the operation of the fan. We can also note, as already highlighted above, that the 270° microphone position shows the greatest energy content at both low and medium frequencies. On the other hand, as already foreseen, the maximum speed of the fan determines a greater acoustic emission, and this occurs both at low and medium frequencies.

3.2. Simulation of Dust Deposits on the Blades of an Axial Fan

As previously said, the goal of this study is to identify the defect using deep learning to identify dust deposits on the blades of an axial fan by the acquisition of the acoustic emission. Two operating conditions have been foreseen: No-Fault, Fault. In the No-Fault condition, the fan blades are perfectly clean and there are no accumulations of material on the surface. In the Fault condition, on the other hand, deposits of material have been artificially created on the fan blades to simulate those which normally deposit over time in the normal operation of the equipment. To simulate the deposits of dust on the fan blades, fine-grained sand (0.1–2 mm) was used, which was made to adhere to the surface of the blades with the use of a thin layer of vinyl glue. The choice of using this granulometry is justified by the need to provide operating conditions in harsh environments such as industrial ones, in which dusty fluids containing abrasive powders are treated. Since it was

found that the deposit is greatest on the leading edges of the fan blade, this aspect was considered in the application of the thin layer of sand.

Figure 7 compares the thermal pictures collected in the two operating situations with the two states of the fan blades.
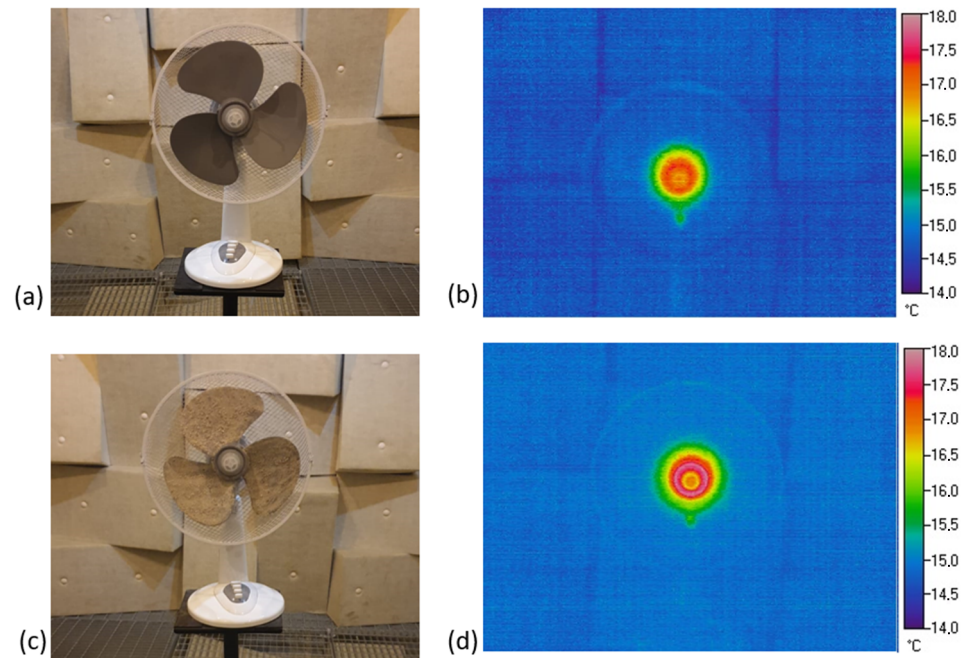

Figure 7. Axial fan in the two operating conditions; (**a**) No-Fault: the fan blades are perfectly clean and there are no accumulations of material on the surface; (**b**) Thermal image of the fan in No-Fault operating conditions; (**c**) Fault: there are deposits of artificially created material on the fan blades; (**b**) Thermal image of the fan in Fault operating conditions.

From the comparison between the thermal images of the fan in the two operating conditions (No-Fault—Figure 7b, Fault—Figure 7d), we can see that the central part of the fan where the rotation axis of the impeller is located shows at higher temperatures due to the heat developed by the frictional forces. In Figure 7d, the axis of rotation appears hotter because of greater friction due to the imbalance caused by deposits of material on the blades. This unbalancing creates additional vibrations on the impeller axis which generate different acoustic emissions compared to normal operating conditions.

3.3. Features Extraction for Acoustics Emissions

For the classification of the operating conditions of the fan we used an algorithm based on 2D CNN: As input we chose to extract spectrograms from the recordings made in the anechoic chamber, for the two operating conditions. This is because CNNs have proven effective in image processing. The abscissa, which measures time, the ordinate, which measures frequency, and the colors, which depict sound intensity, make up the spectrogram. Dark colors depict low-intensity sound in the resulting image, while light hues depict high-intensity sound. The frequency content of a signal's time progression in frequency is returned by the spectrogram.

To ensure there were enough samples for the training and testing phases, each recording was initially divided into segments lasting 5 s. In this manner, 120 samples were removed and divided equally between the two proof of identity classes (No-Fault, Fault). For each sample the spectrogram was calculated, as shown in Figure 7 in which two spectrograms relating to the two operating conditions are compared.

Let us examine two spectrograms for two signals to see how they might be used to determine the fan's operating state. The fan's acoustic emission spectrogram with absolutely

clean blades is displayed in the first signal (Figure 8a), which was created using a sample of the 5 min audio recording. To highlight the frequencies that can discriminate between operating conditions, we have narrowed the frequency range to the 20 Hz–20 kHz range. The second signal shows the spectrogram of the acoustic emission of the fan with blades with artificially created deposits of material (Figure 8b). We can verify that the second signal shows a higher frequency content particularly at low frequencies, representative of the unbalancing of the axis of rotation caused by material deposits. A spectrogram was created for each sample and then saved as an 800×800-pixel png picture.
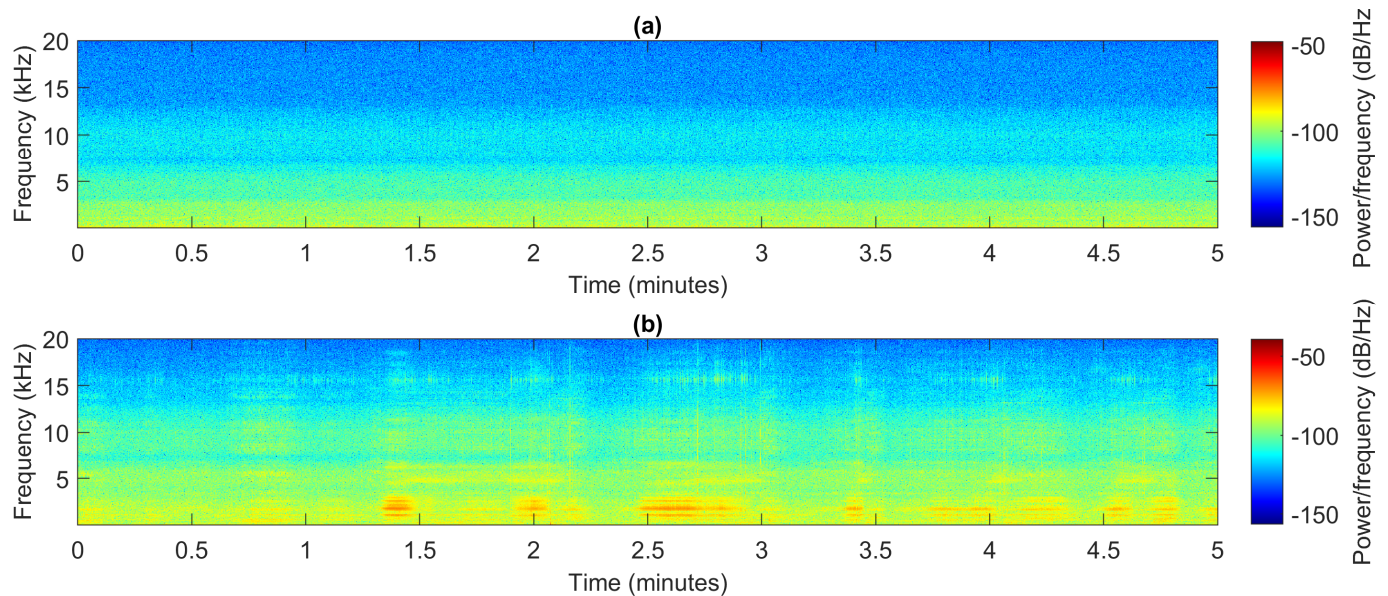
Figure 8. Spectrograms of the two signals: (**a**) No-Fault: the fan blades are perfectly clean and there are no accumulations of material on the surface; (**b**) Fault: there are deposits of artificially created material on the fan blades.

3.4. Fan Fault Diagnosi Using Convolutional Neural Network

To enhance the number of samples to be used in the model training phase, the segmented signal spectrograms were subsequently converted. The transformations have been chosen according to the available samples with the aim of adding information and must not introduce distortions. In this sense, the crop was excluded a priori as it would have stolen useful information, eliminating part of the spectrogram. The objective of this preliminary operation was to maximize the variation of the transformations of the objects within each class and to reduce variance in the same among classes as much as possible. Transformations such as rotation, resizing, and reflection have been made.

Figure 9 shows an example of Image Augmentation application performed on two spectrogram samples relating to the two operating conditions. Data Augmentation enriched the original dataset from 120 samples to 840 samples. The use of Data Augmentation resulted in a slower convergence of the algorithm in the model training phase but returned greater accuracy in the testing phase.
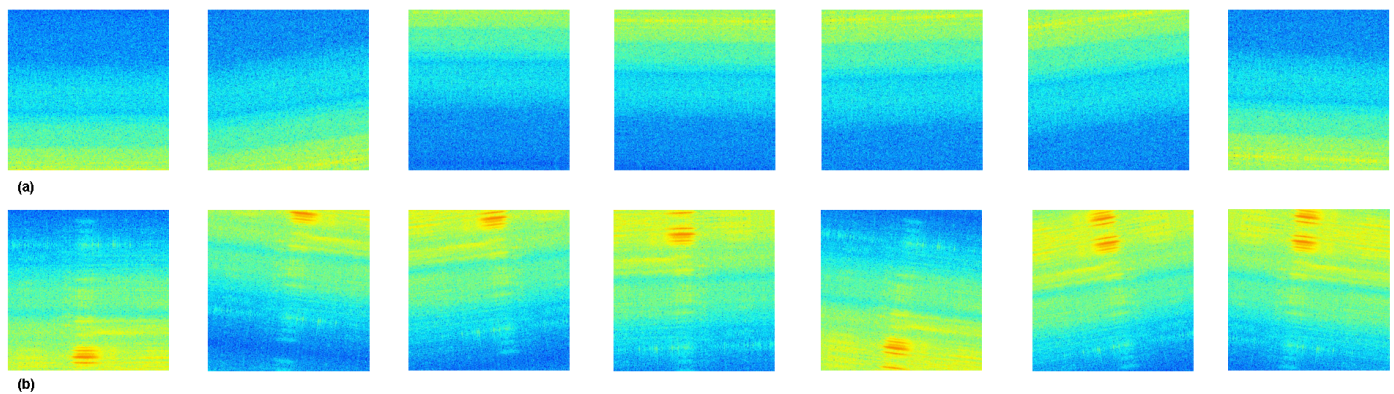
Figure 9. Image augmentation example: In line (**a**), starting from the left, the starting image relating to the No-Fault condition is shown and alongside six transformations of the first image by applying rotation, shift, zoom, horizontal and vertical flip. Line (**b**) shows the starting image relating to the Fault condition and alongside six transformations of the first image by applying rotation, shift, zoom, horizontal and vertical flip.

It was decided to use transfer learning by utilizing a pre-trained network for the recognition of images to take advantage of the small number of samples to be used in the training phase and to shorten the training times required in the case of a network initialized starting from random values.

Several pre-trained models are available in the MATLAB environment from which specialized training can be continued. In this study we used the SqueezeNet model [74], which is a CNN level 18, More than a million photos from the ImageNet database were used to train the network [75]. A picture database called ImageNet is organized using the WordNet hierarchy [76], with thousands of photos serving as representations for each node of the hierarchy. The database has helped deep learning and computer vision research advance. For non-commercial use, the data are freely available to researchers [77]. The pre-trained network has acquired rich representation of features for a variety of photos and can categorize images into 1000 different item categories. The network works on images of dimensions 227 × 227. To be able to adapt it to our problem the settings of the input layer have been modified which has been set to receive images of dimensions 800 × 800, in the queue of the network the Classification layer has been modified to return output with only two classes (No-Fault, Fault).

The use of a pre-trained network allowed us to adapt and transfer the weights of the network to the new data that refer to the acoustic emission detected in the different operating conditions of the fan. Training set and test set were created from the spectrograms that were extracted from the anechoic chamber recordings after being appropriately enhanced. The training set was used to develop the classification model, and the test set was used to assess how well it performed. We have reserved 70% of the available samples (588 spectrograms) equally distributed between No-Fault and Fault events for the training phase. The model performance was evaluated using the remaining 30%, or 252 spectrograms, which were equally split between Fault and No-Fault occurrences.

Table 2 shows the training parameters set.

Table 2. Pre-trained CNN training option.

Solver	Basic	Advanced
sgdm	MaxEpochs = 30	L2Reg = 0.0001
Initial learning rate = 0.01	MiniBatchSize = 1	Grad Threshold Methods = l2norm

The learning phase first involves the initialization of the filters, parameters, and weights; in this phase all the various training options are set also in accordance with the specifications of the available GPU [78].

Then it will be possible to start training the net with the chosen training set. This is a very expensive operation at a computational level: The training phase, as already mentioned, can be omitted as the neural networks offer us different usage scenarios; in fact, in some circumstances it is possible to avoid a computationally expensive training of the network through a Transfer Learning operation with the use of a pre-trained network [79–81]. Using the weights modified during the earlier training and transferred to test a related model, the already trained network is employed for the next job. When utilized as a feature extractor on the data set collected from the ventilator acoustic emission recordings, the pre-trained network (Squeeze Net) was reused after the last layer (completely connected) was removed. The patterns of network accuracy and loss during the training and validation procedure are shown in Figure 10.
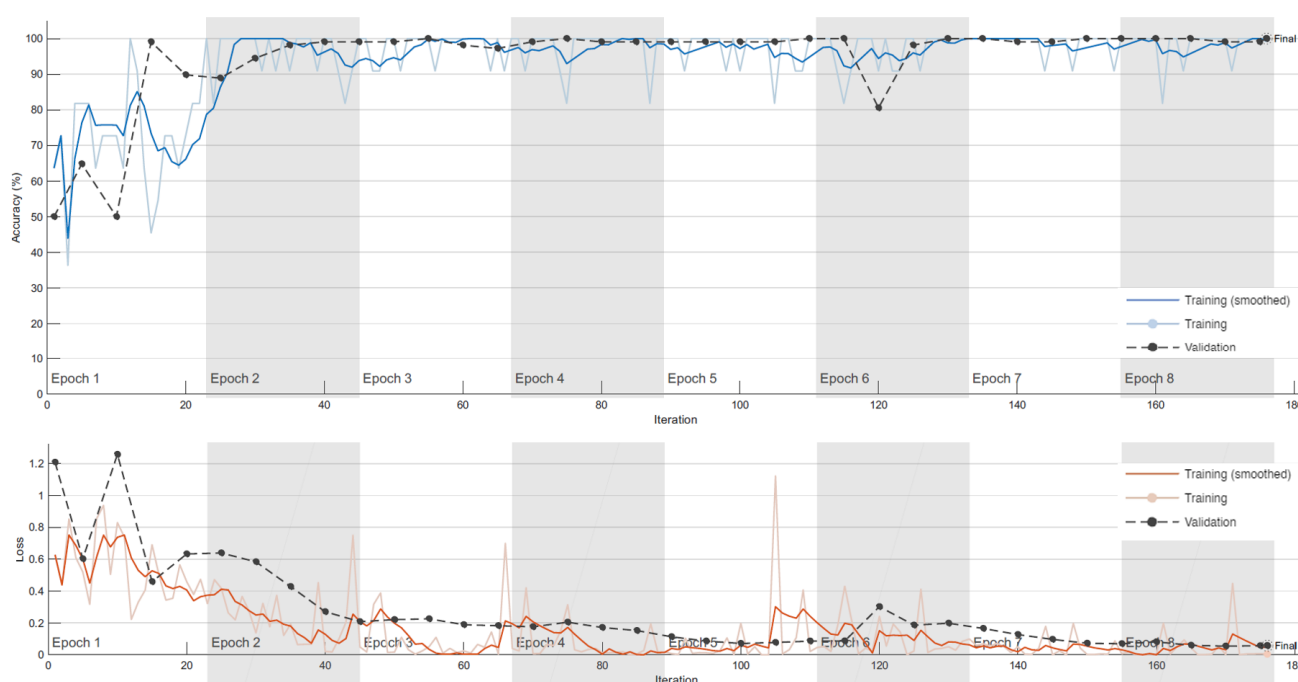

Figure 10. Accuracy and loss in the training and validation phase.

To avoid over-dimensioning issues, the model has been tested using the residual 30% of the data after the network had been trained with 70 percent of the overall of the available data. This ensured that in the test phase the data used had never been seen by the model previously. The model's performance was assessed using accuracy because accuracy is a gauge of how effectively our model works. If our model is accurate, it ought to be nearer to one. The convolutional neural network model produced an accuracy of 0.95, proving the viability of the method for determining the fan's operating settings.

Accuracy provides us with a measure of the correlation between an expected value and a real value, an accurate result means fewer errors in the prediction. Thus, the accuracy of a prediction tells us how close the expected value is to the true value of that quantity. Table 3 shows a comparison between the results obtained in this study and others published by other authors.

Table 3. Machine Learning-based methods for fault diagnosis.

Reference	ML Algorithm	Accuracy
This study	Deep Learning	0.95
[45]	Deep Learning	0.98
[44]	CS-ELM	0.97
[46]	Deep Learning	0.99

Table 3 shows that the results obtained with the present study are in line with those obtained by other researchers. In all the references compared, an accuracy of the method very close to unity is recorded, indicating that the methodology adopted can effectively identify the operating conditions of the fan. The slightly higher accuracy shown by the other studies is essentially because the artificially operated damages to the fan were of greater consistency. These are, in fact, holes made in the blade, injuries or breakage of a blade, conditions that are much more critical than the operating conditions hypothesized in this study.

4. Conclusions

In this study, a new methodology for automating ventilator maintenance procedures was developed. For the detection of dust deposits on the blades of an axial fan, a methodology based on the assessment of the malfunction utilizing deep learning and the collection of the auditory emission was tested. Data relating to the various operating conditions were first collected. Two operating conditions have been identified: No-fault, Fault. In the No-Fault condition, the fan blades are perfectly clean and there are no accumulations of material on the surface. In the Fault condition, on the other hand, deposits of material have been artificially created on the fan blades to simulate those normally found in the normal operation of the equipment. Through a dichotomous classification, the measurements of the fan 660's acoustic emission in the various operating circumstances have been appropriately identified (No-Fault, Fault). The gathered information was utilized to train a convolutional neural network (CNN) algorithm for the automatic recognition of the fan's operating characteristics.

The network was trained using a pre-trained network (Squeeze Net) that was trained on the ImageNet dataset and can categorize objects into up to 1000 different categories. Excellent results were obtained from the Transfer Learning performed on the visuals of the spectrograms obtained from the recording of the fan's sound emission under the two operating conditions. The accuracy of the model tested on the test set returned values very close to unity (0.95) confirming the excellent performance of the methodology. This methodology can be used to automate the maintenance procedures of fans, inserted in industrial processes that deal with dirty fluids, and which have direct access difficulties.

References

1. Mannan, M.; Al-Ghamdi, S.G. Indoor air quality in buildings: A comprehensive review on the factors influencing air pollution in residential and commercial structure. *Int. J. Environ. Res. Public Health* **2021**, *18*, 3276. [CrossRef]
2. Huizenga, C.; Abbaszadeh, S.; Zagreus, L.; Arens, E.A. *Air Quality and Thermal Comfort in Office Buildings: Results of a Large Indoor Environmental Quality Survey*; UC Berkeley: Berkeley, CA, USA, 2006.
3. Lei, L.; Chen, W.; Xue, Y.; Liu, W. A comprehensive evaluation method for indoor air quality of buildings based on rough sets and a wavelet neural network. *Build. Environ.* **2019**, *162*, 106296. [CrossRef]
4. Wyon, D.P. The effects of indoor air quality on performance and productivity. *Indoor Air* **2004**, *14*, 92–101. [CrossRef]
5. Kumar, P.; Martani, C.; Morawska, L.; Norford, L.; Choudhary, R.; Bell, M.; Leach, M. Indoor air quality and energy management through real-time sensing in commercial buildings. *Energy Build.* **2016**, *111*, 145–153. [CrossRef]
6. Salthammer, T. Emerging indoor pollutants. *Int. J. Hyg. Environ. Health* **2020**, *224*, 113423. [CrossRef]
7. Lebowitz, M.D. Health effects of indoor pollutants. *Annu. Rev. Public Health* **1983**, *4*, 203–221. [CrossRef]
8. Pérez-Padilla, R.; Schilmann, A.; Riojas-Rodriguez, H. Respiratory health effects of indoor air pollution. *Int. J. Tuberc. Lung Dis.* **2010**, *14*, 1079–1086.
9. Domínguez-Amarillo, S.; Fernández-Agüera, J.; Cesteros-García, S.; González-Lezcano, R.A. Bad air can also kill: Residential indoor air quality and pollutant exposure risk during the COVID-19 crisis. *Int. J. Environ. Res. Public Health* **2020**, *17*, 7183. [CrossRef]
10. Urrutia-Pereira, M.; Mello-da-Silva, C.A.; Solé, D. Household pollution and COVID-19: Irrelevant association? *Allergol. Et Immunopathol.* **2021**, *49*, 146–149. [CrossRef]
11. Pietrogrande, M.C.; Casari, L.; Demaria, G.; Russo, M. Indoor air quality in domestic environments during periods close to Italian COVID-19 lockdown. *Int. J. Environ. Res. Public Health* **2021**, *18*, 4060. [CrossRef]
12. Dutkiewicz, J.; Cisak, E.; Sroka, J.; Wójcik-Fatla, A.; Zajac, V. Biological agents as occupational hazards-selected issues. *Ann. Agric. Environ. Med.* **2011**, *18*, 286–293.
13. Santos, J.; Ramos, C.; Vaz-Velho, M.; Vasconcelos Pinto, M. Occupational exposure to biological agents. In *International Conference on Applied Human Factors and Ergonomics*; Springer: Cham, Singapore, 2020; pp. 61–67.
14. Kreiss, K. The epidemiology of building-related complaints and illness. *Occup. Med. (Phila. Pa.)* **1989**, *4*, 575–592.
15. Crook, B.; Burton, N.C. Indoor moulds, sick building syndrome and building related illness. *Fungal Biol. Rev.* **2010**, *24*, 106–113. [CrossRef]
16. Redlich, C.A.; Sparer, J.; Cullen, M.R. Sick-building syndrome. *Lancet* **1997**, *349*, 1013–1016. [CrossRef]
17. Burge, P.S. Sick building syndrome. *Occup. Environ. Med.* **2004**, *61*, 185–190. [CrossRef]
18. Bluyssen, P.M.; Cox, C.; Seppänen, O.; de Oliveira Fernandes, E.; Clausen, G.; Müller, B.; Roulet, C.A. Why, when and how do HVAC-systems pollute the indoor environment and what to do about it? The European AIRLESS project. *Build. Environ.* **2003**, *38*, 209–225. [CrossRef]
19. Batterman, S.A.; Burge, H. HVAC systems as emission sources affecting indoor air quality: A critical review. *HVACR Res.* **1995**, *1*, 61–78. [CrossRef]
20. Brief, R.S.; Bernath, T. Indoor pollution: Guidelines for prevention and control of microbiological respiratory hazards associated with air conditioning and ventilation systems. *Appl. Ind. Hyg.* **1988**, *3*, 5–10. [CrossRef]
21. Afram, A.; Janabi-Sharifi, F. Review of modeling methods for HVAC systems. *Appl. Therm. Eng.* **2014**, *67*, 507–519. [CrossRef]
22. McDowall, R. *Fundamentals of HVAC Systems: SI Edition*; Academic Press: Cambridge, MA, USA, 2007.
23. Perez-Lombard, L.; Ortiz, J.; Maestre, I.R. The map of energy flow in HVAC systems. *Appl. Energy* **2011**, *88*, 5020–5031. [CrossRef]
24. Mishra, R.C.; Pathak, K. *Maintenance Engineering and Management*; PHI Learning Pvt. Ltd.: New Delhi, India, 2012.
25. Grigoriev, A.; Van De Klundert, J.; Spieksma, F.C. Modeling and solving the periodic maintenance problem. *Eur. J. Oper. Res.* **2006**, *172*, 783–797. [CrossRef]
26. Envia, E. Fan noise reduction: An overview. *Int. J. Aeroacoustics* **2002**, *1*, 43–64. [CrossRef]
27. Envia, E.; Wilson, A.G.; Huff, D.L. Fan noise: A challenge to CAA. *Int. J. Comput. Fluid Dyn.* **2004**, *18*, 471–480. [CrossRef]
28. Filleul, N.L.S. An investigation of axial flow fan noise. *J. Sound Vib.* **1966**, *3*, 147–165. [CrossRef]
29. Woodward, R.; Hughes, C.; Jeracki, R.; Miller, C. Fan Noise Source Diagnostic Test–Far-field Acoustic Results. In Proceedings of the 8th AIAA/CEAS Aeroacoustics Conference & Exhibit, Breckenridge, CO, USA, 17–19 June 2002; p. 2427. [CrossRef]
30. Hughes, C.; Jeracki, R.; Woodward, R.; Miller, C. Fan noise source diagnostic test-rotor alone aerodynamic performance results. In Proceedings of the 8th AIAA/CEAS Aeroacoustics Conference & Exhibit, Breckenridge, CO, USA, 17–19 June 2002; p. 2426.
31. Iannace, G.; Ciaburro, G.; Trematerra, A. Fault diagnosis for UAV blades using artificial neural network. *Robotics* **2019**, *8*, 59. [CrossRef]
32. Kankar, P.K.; Sharma, S.C.; Harsha, S.P. Fault diagnosis of ball bearings using machine learning methods. *Expert Syst. Appl.* **2011**, *38*, 1876–1886. [CrossRef]
33. Ciaburro, G. Machine fault detection methods based on machine learning algorithms: A review. *Math. Biosci. Eng.* **2022**, *19*, 11453–11490. [CrossRef]
34. Aldrich, C.; Auret, L. *Unsupervised Process Monitoring and Fault Diagnosis with Machine Learning Methods*; Springer: London, UK, 2013; Volume 16, pp. 593–606.
35. Mitchell, T.M.; Mitchell, T.M. *Machine Learning*; McGraw-Hill: New York, NY, USA, 1997; Volume 1.

36. Ciaburro, G.; Iannace, G.; Puyana-Romero, V.; Trematerra, A. A comparison between numerical simulation models for the prediction of acoustic behavior of giant reeds shredded. *Appl. Sci.* **2020**, *10*, 6881. [CrossRef]
37. Janiesch, C.; Zschech, P.; Heinrich, K. Machine learning and deep learning. *Electron. Mark.* **2021**, *31*, 685–695. [CrossRef]
38. Puyana-Romero, V.; Ciaburro, G.; Brambilla, G.; Garzón, C.; Maffei, L. Representation of the soundscape quality in urban areas through colours. *Noise Mapp.* **2019**, *6*, 8–21. [CrossRef]
39. Mahesh, B. Machine learning algorithms—A review. *Int. J. Sci. Res.* **2020**, *9*, 381–386.
40. Ciaburro, G.; Iannace, G. Machine learning-based algorithms to knowledge extraction from time series data: A review. *Data* **2021**, *6*, 55. [CrossRef]
41. Lei, Y.; Yang, B.; Jiang, X.; Jia, F.; Li, N.; Nandi, A.K. Applications of machine learning to machine fault diagnosis: A review and roadmap. *Mech. Syst. Signal Process.* **2020**, *138*, 106587. [CrossRef]
42. Guo, L.; Lei, Y.; Xing, S.; Yan, T.; Li, N. Deep convolutional transfer learning network: A new method for intelligent fault diagnosis of machines with unlabeled data. *IEEE Trans. Ind. Electron.* **2018**, *66*, 7316–7325. [CrossRef]
43. Chen, Z.; Gryllias, K.; Li, W. Mechanical fault diagnosis using convolutional neural networks and extreme learning machine. *Mech. Syst. Signal Process.* **2019**, *133*, 106272. [CrossRef]
44. Xu, Y.; Chen, N.; Shen, X.; Xu, L.; Pan, Z.; Pan, F. Proposal and experimental case study on building ventilating fan fault diagnosis based on cuckoo search algorithm optimized extreme learning machine. *Sustain. Energy Technol. Assess.* **2021**, *45*, 100975. [CrossRef]
45. Huang, G.; Qiao, L.; Khanna, S.; Pavlovich, P.A.; Tiwari, S. Research on fan vibration fault diagnosis based on image recognition. *J. Vibroeng.* **2021**, *23*, 1366–1382. [CrossRef]
46. Zhang, T.; Xu, F.; Jia, M. A centrifugal fan blade damage identification method based on the multi-level fusion of vibro-acoustic signals and CNN. *Measurement* **2022**, *199*, 111475. [CrossRef]
47. Xie, X.; Chen, W.; Chen, B.; Cheng, J.; Tan, L. Comprehensive fatigue estimation and fault diagnosis based on Refined Generalized Multi-Scale Entropy method of centrifugal fan blades. *Measurement* **2020**, *166*, 108224. [CrossRef]
48. Choudhary, A.; Goyal, D.; Letha, S.S. Infrared thermography-based fault diagnosis of induction motor bearings using machine learning. *IEEE Sens. J.* **2020**, *21*, 1727–1734. [CrossRef]
49. Hsu, J.Y.; Wang, Y.F.; Lin, K.C.; Chen, M.Y.; Hsu, J.H.Y. Wind turbine fault diagnosis and predictive maintenance through statistical process control and machine learning. *IEEE Access* **2020**, *8*, 23427–23439. [CrossRef]
50. Rauber, T.W.; da Silva Loca, A.L.; de Assis Boldt, F.; Rodrigues, A.L.; Varejão, F.M. An experimental methodology to evaluate machine learning methods for fault diagnosis based on vibration signals. *Expert Syst. Appl.* **2021**, *167*, 114022. [CrossRef]
51. Ibrahim, S.K.; Ahmed, A.; Zeidan, M.A.E.; Ziedan, I.E. Machine learning techniques for satellite fault diagnosis. *Ain Shams Eng. J.* **2020**, *11*, 45–56. [CrossRef]
52. Doe, U. Improving Fan System Performance: A Sourcebook for Industry. Prepared by Lawrence Berkeley National Laboratory and Resource Dynamics Corporation, Washington. Washington. Technical Report, DC DOE/GO-102003-1294. 2003. Available online: https://www.nrel.gov/docs/fy03osti/29166.pdf (accessed on 17 December 2022).
53. Liddament, M.W. GV: A Guide to Energy Efficient Ventilation. 1996. Available online: https://www.aivc.org/resource/gv-guide-energy-efficient-ventilation?utm_medium=website&utm_source=archdaily.com.br (accessed on 17 December 2022).
54. Santamouris, M.; Wouters, P. *Building Ventilation: The State of the Art*; Routledge: Oxfordshire, UK, 2015.
55. Estill, C.F.; Watkins, D.S.; Hall, R.M.; O'Brien, D.M.; Shulman, S.A. The impact of maintenance and design for ventilation systems. *Appl. Occup. Environ. Hyg.* **2002**, *17*, 344–351. [CrossRef]
56. *ISO 3745 Standard*; Acoustics—Determination of Sound Power Levels of Noise Sources Using Sound Pressure Precision Methods for Anechoic and Hemi-Anechoic Rooms. ISO: Geneva, Switzerland, 2012.
57. Guyon, I.; Gunn, S.; Nikravesh, M.; Zadeh, L.A. (Eds.) *Feature Extraction: Foundations and Applications*; Springer: Berlin/Heidelberg, Germany, 2008; Volume 207.
58. Sakashita, Y.; Aono, M. Acoustic scene classification by ensemble of spectrograms based on adaptive temporal divisions. In *Detection and Classification of Acoustic Scenes and Events (DCASE) Challenge*; DCASE Community: Washington, DC, USA, 2018.
59. Ciaburro, G. Sound event detection in underground parking garage using convolutional neural network. *Big Data Cogn. Comput.* **2020**, *4*, 20. [CrossRef]
60. Harčarik, T.; Bocko, J.; Masláková, K. Frequency analysis of acoustic signal using the Fast Fourier Transformation in MATLAB. *Procedia Eng.* **2012**, *48*, 199–204. [CrossRef]
61. Shin, M.; Hong, W.; Lee, K.; Choo, Y. Frequency Analysis of Acoustic Data Using Multiple-Measurement Sparse Bayesian Learning. *Sensors* **2021**, *21*, 5827. [CrossRef]
62. Ciaburro, G.; Iannace, G. Machine-Learning-Based Methods for Acoustic Emission Testing: A Review. *Appl. Sci.* **2022**, *12*, 10476. [CrossRef]
63. Gu, J.; Wang, Z.; Kuen, J.; Ma, L.; Shahroudy, A.; Shuai, B.; Chen, T. Recent advances in convolutional neural networks. *Pattern Recognit.* **2018**, *77*, 354–377. [CrossRef]
64. Albawi, S.; Mohammed, T.A.; Al-Zawi, S. Understanding of a convolutional neural network. In Proceedings of the 2017 International Conference on Engineering and Technology (ICET), Nagoya, Japan, 21–23 August 2017; IEEE: Piscataway, NJ, USA; pp. 1–6. [CrossRef]

65. Wu, J. Introduction to convolutional neural networks. National Key Lab for Novel Software Technology. *Nanjing Univ.* **2017**, *5*, 495.

66. Shorten, C.; Khoshgoftaar, T.M. A survey on image data augmentation for deep learning. *J. Big Data* **2019**, *6*, 60. [CrossRef]

67. Taylor, L.; Nitschke, G. Improving deep learning with generic data augmentation. In Proceedings of the 2018 IEEE Symposium Series on Computational Intelligence (SSCI), Bangalore, India, 18–21 November 2018; IEEE: Piscataway, NJ, USA; pp. 1542–1547.

68. Wang, J.; Perez, L. The effectiveness of data augmentation in image classification using deep learning. *Convolutional Neural Netw. Vis. Recognit* **2017**, *11*, 1–8.

69. Li, X.; Zhang, W.; Ding, Q.; Sun, J.Q. Intelligent rotating machinery fault diagnosis based on deep learning using data augmentation. *J. Intell. Manuf.* **2020**, *31*, 433–452. [CrossRef]

70. Bengio, Y. Deep learning of representations for unsupervised and transfer learning. In Proceedings of the ICML Workshop on Unsupervised and Transfer Learning, JMLR Workshop and Conference Proceedings, Bellevue, Washington, USA, 2 July 2011; pp. 17–36.

71. Tan, C.; Sun, F.; Kong, T.; Zhang, W.; Yang, C.; Liu, C. A survey on deep transfer learning. In Proceedings of the International Conference on Artificial Neural Networks, 2018 October; Springer: Cham, Singapore; pp. 270–279.

72. Zhuang, F.; Qi, Z.; Duan, K.; Xi, D.; Zhu, Y.; Zhu, H.; He, Q. A comprehensive survey on transfer learning. *Proc. IEEE* **2020**, *109*, 43–76. [CrossRef]

73. Shao, S.; McAleer, S.; Yan, R.; Baldi, P. Highly accurate machine fault diagnosis using deep transfer learning. *IEEE Trans. Ind. Inform.* **2018**, *15*, 2446–2455. [CrossRef]

74. Iandola, F.N.; Han, S.; Moskewicz, M.W.; Ashraf, K.; Dally, W.J.; Keutzer, K. SqueezeNet: AlexNet-level accuracy with 50x fewer parameters and <0.5 MB model size. *arXiv preprint* **2016**, arXiv:1602.07360.

75. Russakovsky, O.; Deng, J.; Su, H.; Krause, J.; Satheesh, S.; Ma, S.; Fei-Fei, L. Imagenet large scale visual recognition challenge. *Int. J. Comput. Vis.* **2015**, *115*, 211–252. [CrossRef]

76. Miller, G.A. WordNet: A lexical database for English. *Commun. ACM* **1995**, *38*, 39–41. [CrossRef]

77. Yang, K.; Qinami, K.; Fei-Fei, L.; Deng, J.; Russakovsky, O. Towards fairer datasets: Filtering and balancing the distribution of the people subtree in the imagenet hierarchy. In Proceedings of the 2020 Conference on Fairness, Accountability, and Transparency, Barcelona, Spain, 27–30 January 2020; pp. 547–558. [CrossRef]

78. LeCun, Y.; Bengio, Y.; Hinton, G. Deep learning. *Nature* **2015**, *521*, 436–444. [CrossRef]

79. Goodfellow, I.; Bengio, Y.; Courville, A. *Deep Learning*; MIT Press: Cambridge, MA, USA, 2016.

80. Iannace, G.; Ciaburro, G. Modelling sound absorption properties for recycled polyethylene terephthalate-based material using Gaussian regression. *Build. Acoust.* **2021**, *28*, 185–196. [CrossRef]

81. Guo, Y.; Liu, Y.; Oerlemans, A.; Lao, S.; Wu, S.; Lew, M.S. Deep learning for visual understanding: A review. *Neurocomputing* **2016**, *187*, 27–48. [CrossRef]